

Manufactured Silver Nanoparticles of Different Sizes Induced DNA Strand Breaks and Oxidative DNA Damage in Hepatoma and Leukaemia Cells and in Dermal and Pulmonary Fibroblasts

(comet assay / DNA strand breaks / genotoxicity / human cell lines / oxidative DNA damage / silver nanoparticles)

A. ÁVALOS, A. I. HAZA, P. MORALES

Departamento de Nutrición, Bromatología y Tecnología de los Alimentos. Facultad de Veterinaria, Universidad Complutense de Madrid, Spain

Abstract. Many classes of silver nanoparticles (AgNPs) have been synthesized and widely applied, but no conclusive information on their potential cytotoxicity and genotoxicity mechanisms is available. Therefore, the purpose of this study was to compare the potential genotoxic effects (DNA strand breaks and oxidative DNA damage) of 4.7 nm coated and 42 nm uncoated AgNPs, using the comet assay, in four relevant human cell lines (hepatoma, leukaemia, and dermal and pulmonary fibroblasts) in order to understand the impact of such nanomaterials on cellular DNA. The results indicated that in all cell lines tested, 4.7 nm coated ($0.1\text{--}1.6\ \mu\text{g ml}^{-1}$) and 42 nm uncoated ($0.1\text{--}6.7\ \mu\text{g ml}^{-1}$) AgNPs increased DNA strand breaks in a dose- and size-dependent manner following 24 h treatment, the smaller AgNPs being more genotoxic. Human pulmonary fibroblasts showed the

highest sensitivity to the AgNPs. A modified comet assay using endonuclease III and formamidopyrimidine-DNA glycosylase restriction enzymes showed that in tumoral and normal human dermal fibroblasts, pyrimidines and purines were oxidatively damaged by both AgNPs, but the damage was not size-dependent. However, in human pulmonary fibroblasts, no oxidative damage was observed after treatment with 42 nm AgNPs. In conclusion, both AgNP sizes induced DNA damage in human cells, and this damage could be related to oxidative stress.

Introduction

Nanoparticles (NPs), which are defined as particles having at least one dimension of 100 nm or less, are used to produce nanomaterials (Maynard and Kuempel, 2005). Materials at this scale typically exhibit nanostructure-dependent properties, such as unique physical properties (optical, electrical, and magnetic) and highly chemical reactivity, which make them more attractive for commercial and medical applications (Oberdörster et al., 2005). For example, these nanomaterials are used in bioapplications as therapeutics, transfection vectors and fluorescent labels (Tan et al., 2007; Yoon et al., 2007; Kreuter and Gelperina, 2008; Su et al., 2008). However, the novel physicochemical properties of nanoscale materials emphasize the need for proper assessment of their potential effects on human health. The main feature of these nanomaterials is that in comparison with bulk materials, NPs possess a higher surface-to-volume ratio and thus an enhanced contact area with their surroundings than do bulk materials at the same mass (Maurer-Jones et al., 2010). Their small size, high surface area per unit mass, chemical composition, and surface property effects may be important factors in NP-induced toxicity (Wallace et al., 2007) and nonspecific oxidative damage is one of the greatest concerns (Colvin, 2003; Nel et al., 2006; Xia et al., 2006).

Received July 23, 2014. Accepted November 13, 2014.

This work has been supported by Grant AGL2010-16561 from the Ministerio de Educación, Cultura y Deporte (Spain). A. Ávalos is a recipient of a fellowship from the Ministerio de Educación, Cultura y Deporte, Spain.

Corresponding author: Paloma Morales, Department of Nutrición, Bromatología y Tecnología de los Alimentos, Faculty of Veterinary, Complutense University of Madrid, Madrid, Spain. Phone: (+34) 91-394 37 47; Fax: (+34) 91-394 37 43; e-mail: pmmorales@vet.ucm.es.

Abbreviations: AgNPs – silver nanoparticles, DLS – dynamic light scattering, Endo III – endonuclease III, Fpg – formamidopyrimidine-DNA glycosylase, HepG2 – hepatoma cells, HL-60 – leukaemia cells, HPF – human pulmonary fibroblasts, LDH – lactate dehydrogenase, MNF – micronucleation frequency, MTT – 3-(4,5-dimethylthiazol-2-yl)-2,5-diphenyltetrazolium bromide, NHDF – normal human dermal fibroblasts, NPs – nanoparticles, PEI – polyetherimide, PVP – polyvinylpyrrolidone, ROS – reactive oxygen species, SD – standard deviation, SOD – superoxide dismutase, TEM – transmission electron microscopy.

Among the metallic nanomaterials, silver nanoparticles (AgNPs), owing to their anti-microbial potential, are the most commercialized NPs according to the Woodrow-Wilson database, which is a data source for information on products based on nanotechnology. AgNPs are currently exploited within a number of diverse products including electronics, cosmetics, household appliances, textiles and food production, as well as in medical products (Wijnhoven et al., 2009).

As a result of these applications, exposure to AgNPs is becoming increasingly widespread. Despite growing concerns, little is known about the potential impacts of AgNPs on human and environmental health.

For individuals, there are several possible ways to be exposed to AgNPs including dermal contact, oral administration, inhalation, intravenous injection, etc. (Chen and Schluesener, 2008; Ahamed et al., 2010; He et al., 2012). The human body has several semi-open interfaces for direct substance exchange with the environment, i.e. the respiratory tract, gastrointestinal tract and skin. At these sites, nanoparticle can undergo a series of processes such as binding and reacting with proteins, phagocytosis, deposition, clearance and translocation (Mukherjee et al., 2012). Thus, it is important to investigate the toxicity of AgNPs in relevant human tissues.

In this study we used the comet assay, because it is able to detect early DNA breakage with more sensitivity than conventional techniques such as 4',6-diamidino-2-phenylindole staining and DNA flow cytometry (Olive et al., 1993; Godard et al., 1999). It is also one of the most widely used tests and gives the most positive outcome for determining NP genotoxicity. In the present work, the comet assay was also modified to permit detection of oxidized bases by including a step in which DNA is digested with formamidopyrimidine-DNA glycosylase (Fpg) and endonuclease III (Endo III) to uncover oxidized purines and pyrimidines, respectively. Thus, Fpg and Endo III enzymes were used to determine the role of oxidative DNA damage in AgNP genotoxicity. Fpg was selected for its ability to recognize imidazole-ring-opened purines, or formamidopyrimidines (fapy Ade and fapy Gua), which occur during the spontaneous breakdown of damaged purines; however, a major substrate in cellular DNA is 8-oxoGua (Boiteux, 1993). Endo III, acting as a glycosylase, recognizes a variety of oxidized pyrimidines in DNA and removes them, leaving an apurinic/apyrimidinic site (AP-site); and associated AP-endonuclease activity then creates a break in the DNA (Doetsch et al., 1987).

Despite all published studies, determination of the trend of silver nanoparticle toxicity (cytotoxicity and genotoxicity) may be considered complex owing to the different kinds of nanoparticle synthesis, their various sizes, the presence or absence of capping agents, and finally the diverse kinds of toxicity evaluation tests (Lima et al., 2012). Therefore, the European Commission (2012) has reported the necessity to perform determination of the risk of nanomaterials case by case.

The main goal of the present work was thus to compare the potential genotoxic effects (DNA strand breaks and oxidative DNA damage) of 4.7 nm coated AgNPs and 42 nm uncoated AgNPs, using the comet assay, in four relevant human cell lines (hepatoma, leukaemia, dermal and pulmonary fibroblasts) in order to understand the impact of such nanomaterials on cellular DNA.

Material and Methods

Chemicals

All chemicals were reagent grade or higher and were obtained from Sigma-Aldrich (St. Louis, MO), unless otherwise specified. Water-based solutions of 4.7 nm PEI (polyetherimide) and PVP (polyvinylpyrrolidone) coated silver nanoparticles (AgNPs) and 42 nm uncoated AgNPs were purchased from Nanogap Subparticles (A Coruña, Spain). The summary of the characteristics according to the manufacturer's data is available in Table 1. Stock solutions of AgNPs were diluted to the required concentrations using the respective cell culture medium. In order to reduce agglomeration, the suspensions were mixed using a vortex for 20 s and sonicated for 2×20 s with a pause in between using a sonicator probe.

Nanoparticle characterization

Characterization of AgNPs concerning their primary sizes, morphology, agglomeration and size distribution in aqueous solution, and after incubation in cell-free culture media by transmission electron microscopy (TEM) and dynamic light scattering (DLS), was conducted in previous studies (Ávalos et al., 2014a, b).

Cell culture

Tumoral human leukaemia cells (HL-60) and human hepatoma cells (HepG2) were obtained from the Biology Investigation Centre Collection (BIC, Madrid, Spain). HL-60 cells were maintained in RPMI 1640 medium and HepG2 cells were cultured as a monolayer in

Table 1. Characteristics of AgNPs obtained from NanoGap. Nd – no information provided

| Code | Particles | Avg* \pm SD (nm) | Dispersion solution | Density (g/ml) | Density of particles (part/l) | Colour | pH |
|--------|-----------|--------------------|-----------------------------------|----------------|-------------------------------|------------------------------|-----|
| 2106-W | AgNP 4.7 | 4.7 \pm 1 | Aqueous solution with PEI and PVP | 1.024 | 1.75×10^{19} | Black, yellow (when diluted) | 9.3 |
| 2103-W | AgNP 42 | 42 \pm 9 | Aqueous solution | 1.01 | Nd | Brown | Nd |

* As provided by the company, PEI – polyetherimide, PVP – polyvinylpyrrolidone

Dulbecco's modified Eagle's medium. The media were supplemented with 10% v/v heat-inactivated foetal calf serum, 50 µg/ml streptomycin, 50 UI/ml penicillin and 1% v/v L-glutamine. Culture medium and supplements required for the growth of the human tumoral cell lines were purchased from GIBCO (Laboratories Life Technologies Inc., Gaithersburg, MD).

Normal human dermal fibroblasts (NHDF) and human pulmonary fibroblasts (HPF) were purchased from commercial PromoCell GmbH (Heidelberg, Germany). NHDF and HPF were cultured as a monolayer in fibroblast basal medium supplemented with 2% v/v foetal calf serum, 1 ng/ml basic fibroblast growth factor and 5 µg/ml insulin. Culture medium and supplements were purchased from PromoCell GmbH.

All human cell cultures were incubated at 37 °C and 100% humidity in a 5% CO₂ atmosphere.

Analysis of DNA strand breaks induced by AgNPs by alkaline comet assay

The comet assay is based on the microscopic detection of damaged DNA fragments of individual cells, appearing as "comets" upon cell lysis, subsequent DNA denaturation and electrophoresis. To evaluate the DNA damage by AgNPs in tumoral and non-tumoral cells, we performed the comet assay as described by Olive et al. (1992). Previously, in our laboratory, cell viability after exposure to AgNPs 4.7 and 42 nm was routinely determined by the MTT (3-(4,5-dimethylthiazol-2-yl)-2,5-diphenyltetrazolium bromide) and LDH (lactate dehydrogenase) assays in HepG2, HL-60, NHDF and HPF in order to select non-toxic concentrations. The AgNPs of 4.7 nm and 42 nm showed to be cytotoxic in concentrations higher than 1.68 and 6.7 µg ml⁻¹, respectively (Ávalos et al., 2014a, b). For this reason, the concentration ranges of 0.1–1.6 µg ml⁻¹ (AgNPs 4.7 nm) and 0.1–6.7 µg ml⁻¹ (AgNPs 42 nm) were used in genotoxicity studies. Briefly, HepG2, NHDF and HPF cells were plated in multi-well systems at a density of 1.5 × 10⁵ cell ml⁻¹ culture medium; 24 h after seeding, different concentrations of AgNPs of 4.7 (0.1–1.6 µg ml⁻¹) and 42 nm (0.1–6.7 µg ml⁻¹) were added to the wells and the plates were incubated for 24 h at 37 °C and 5% CO₂. After incubation, 10 µl of a suspension of 1.5 × 10⁵ cells was mixed with 70 µl of LPM agarose type VII (0.75% concentration in PBS) distributed on slides that had been pre-coated with LMP agarose type VII (0.30% concentration in PBS), and left to set on an ice tray. Three slides were prepared for each concentration of the AgNPs tested.

After solidification, the cells were lysed in the dark for 1 h in a high-salt alkaline buffer (2.5 M NaCl, 0.1 M EDTA, 0.01 M Tris, 1% Triton X-100, pH 10). The slides were then equilibrated 3 × 5 min in enzyme buffer (0.04 M HEPES, 0.1 M KCl, 0.5 mM EDTA, 0.2 mg ml⁻¹ BSA, pH 8). After that, the slides were placed in electrophoresis buffer (0.3 M NaOH, 1 mM EDTA, pH 13, cooled in a refrigerator) in the dark for 40 min. Electrophoresis was performed in a cold-storage room in the dark, in a Bio-Rad subcell GT unit containing the same buffer, for 30 min at 25 V. After electrophoresis, the slides were neutralized using 0.4 M Tris pH 7.5 and fixed in methanol. Subsequently, the DNA was stained with ethidium bromide (10 µg ml⁻¹) in Tris-acetate EDTA (TAE 1X) for 5 min and examined in a fluorescence microscope (Axiostar plus microscope, Zeiss, NY, NY) connected to a computerized image analysis system (Comet Score, 1.0). Percent (%) DNA in the tail, defined as the fraction of DNA in the tail divided by the total amount of DNA associated with a cell multiplied by 100, was used as the parameter for DNA damage analysis using the software. In experiments with HL-60 cells, the plates were incubated with 1 × 10⁶ cells in complete culture medium, and 500 µl of each of the different concentrations of AgNPs was added to each well. The plates were then incubated for 24 h at 37 °C and 5% CO₂ and processed as described above. Benzo(a)pyrene (100 mM) was used as positive control.

rophoresis was performed in a cold-storage room in the dark, in a Bio-Rad subcell GT unit containing the same buffer, for 30 min at 25 V. After electrophoresis, the slides were neutralized using 0.4 M Tris pH 7.5 and fixed in methanol. Subsequently, the DNA was stained with ethidium bromide (10 µg ml⁻¹) in Tris-acetate EDTA (TAE 1X) for 5 min and examined in a fluorescence microscope (Axiostar plus microscope, Zeiss, NY, NY) connected to a computerized image analysis system (Comet Score, 1.0). Percent (%) DNA in the tail, defined as the fraction of DNA in the tail divided by the total amount of DNA associated with a cell multiplied by 100, was used as the parameter for DNA damage analysis using the software. In experiments with HL-60 cells, the plates were incubated with 1 × 10⁶ cells in complete culture medium, and 500 µl of each of the different concentrations of AgNPs was added to each well. The plates were then incubated for 24 h at 37 °C and 5% CO₂ and processed as described above. Benzo(a)pyrene (100 mM) was used as positive control.

Analysis of oxidative DNA damage induced by AgNPs by modified comet assay

Oxidatively damaged bases can also be detected with the comet assay by adding another step: after lysis, the DNA is digested with Fpg or Endo III to uncover oxidized purines and pyrimidines. The slides were incubated with 30 µl of Fpg and Endo III at 1 µg ml⁻¹ in enzyme buffer for 30 min at 37 °C in a humid dark chamber. Control slides were incubated with 30 µl enzyme buffer only. DNA treated with Endo III nicks the DNA at sites of oxidized pyrimidines, and Fpg recognizes, e.g., 8-oxodG and FAPydg, thereby increasing the number of DNA breaks (Collins et al., 1993). Then, the assay continued as described above. The levels of Fpg and Endo III sites were obtained by subtracting the value of % DNA in the tail obtained without added enzymes from the value when the enzymes were present. Benzo(a)pyrene (100 mM) incubated with Endo III and Fpg enzymes was also used as positive control.

Statistical analyses of data

Images of 50 randomly selected cells per concentration were evaluated and the test was carried out three times. The reported % DNA in the tail is the mean ± standard deviation (SD) of three independent experiments. Cultures without AgNPs were considered as negative controls and cultures with benzo(a)pyrene as positive controls. Student's *t*-test was used for statistical comparison and differences were considered significant at $P \leq 0.05$.

Results

DNA strand breaks by AgNPs

The alkaline comet assay was used to determine the DNA damage associated with exposure to non-cytotoxic

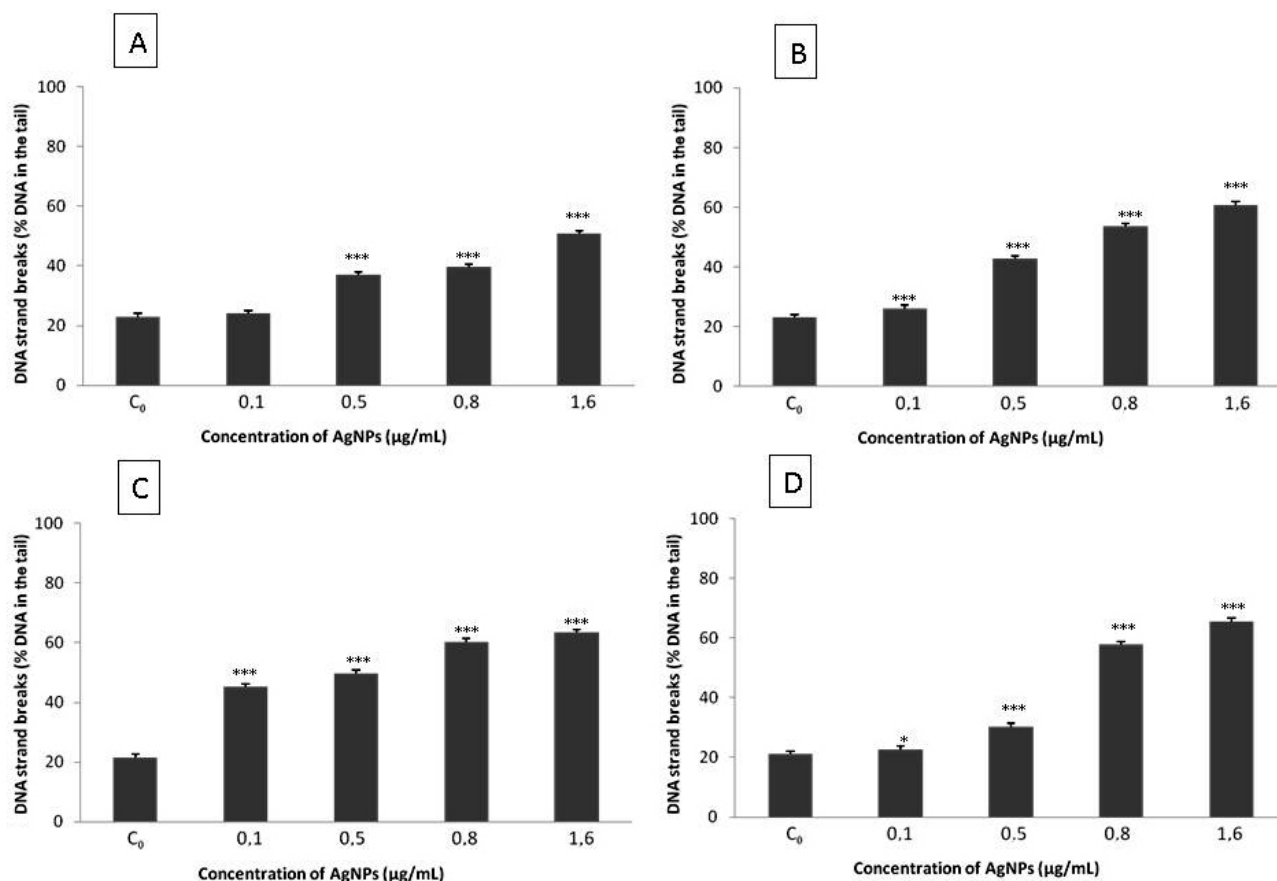


Fig. 1. DNA strand breaks in HepG2 (A), HL-60 (B), NHDF (C) and HPF (D) cells exposed to AgNPs of 4.7 nm, as determined by comet assay. The results are expressed as the mean \pm SD of three independent experiments for data point of the % DNA in the tail of cells. C₀ – untreated cells without enzymes.

Asterisks indicate significant difference from the control *** $P \leq 0.001$, * $P \leq 0.05$.

concentrations of 4.7 nm coated AgNPs (0.1–1.6 $\mu\text{g ml}^{-1}$) and 42 nm uncoated AgNPs (0.1–6.7 $\mu\text{g ml}^{-1}$) in HepG2, HL-60, NHDF and HPF cells. A significant and dose-dependent increase in DNA migration was detected after 24 h of exposure in all cell types. The percentage of DNA in the tail was higher than control at all concentrations.

In HepG2 cells, 4.7 nm coated AgNPs induced a statistically significant increase in DNA strand breaks at concentrations of 0.5–1.6 $\mu\text{g ml}^{-1}$ (37.1–50.8% tail) (Fig. 1A). In all the other cell lines, HL-60, NHDF and HPF, 4.7 nm coated AgNPs were also able to increase the percentage of DNA in the tail significantly at all tested doses, from 0.1–1.6 $\mu\text{g ml}^{-1}$ (26.2–60.8% tail, Fig. 1B; 45.2–63.5% tail, Fig. 1C and 22.7–65.6% tail, Fig. 1D, respectively).

Figure 2 shows DNA damage induced by 42 nm uncoated AgNPs in HepG2, HL-60, NHDF and HPF cells. HepG2 cells were the most resistant to the treatment of AgNPs of 42 nm; a significant increase of DNA strand breaks was only observed at concentrations of 1.6 and 6.7 $\mu\text{g ml}^{-1}$ (40.1% and 61.4% tail, respectively) (Fig. 2A). However, HL-60 cells were the most sensitive, since increased DNA amount was observed in the tail at all concentrations tested, from 0.1–6.7 $\mu\text{g ml}^{-1}$ (26.2–65.4% tail) (Fig. 2B). Finally, NHDF and HPF cells

showed significant DNA damage from 0.5–6.7 $\mu\text{g ml}^{-1}$ (39.7–64.7% and 25.7–67.8% tail, respectively) (Fig. 2C, D).

Comparing DNA damage induced by both AgNP sizes at the same concentration (1.6 $\mu\text{g ml}^{-1}$), small coated AgNPs were more genotoxic than the large uncoated ones in all cell lines. In HepG2 cells, small coated AgNPs induced 50.8 % DNA in the tail, whereas the large uncoated ones only 40.1 %. The percentage of DNA in the tail induced by 4.7 nm AgNPs and 42 nm in HL-60 cells was 60.8 and 44.6 %, respectively. Finally, in NHDF and HPF, 4.7 nm AgNPs induced 63.5 % and 65.6 % DNA in the tail, respectively, whereas the large AgNPs only 45.5 % and a 55 % DNA.

The results of benzo(a)pyrene (100 mM) induced DNA strand breaks were \sim 2.24 (HepG2), 2.87 (HL-60), 2.44 (NHDF) and 3.18 (HPF) fold higher than the background values (data not shown).

Oxidative DNA damage by AgNPs

In order to identify the oxidative DNA damage induced by 4.7 and 42 nm AgNP treatment, two repair-specific enzymes (Fpg and Endo III) that recognize and cut oxidized DNA bases were employed. In HepG2 cells (Fig. 3), the treatment with 4.7 nm coated AgNPs at all tested doses did not cause any significant increase of

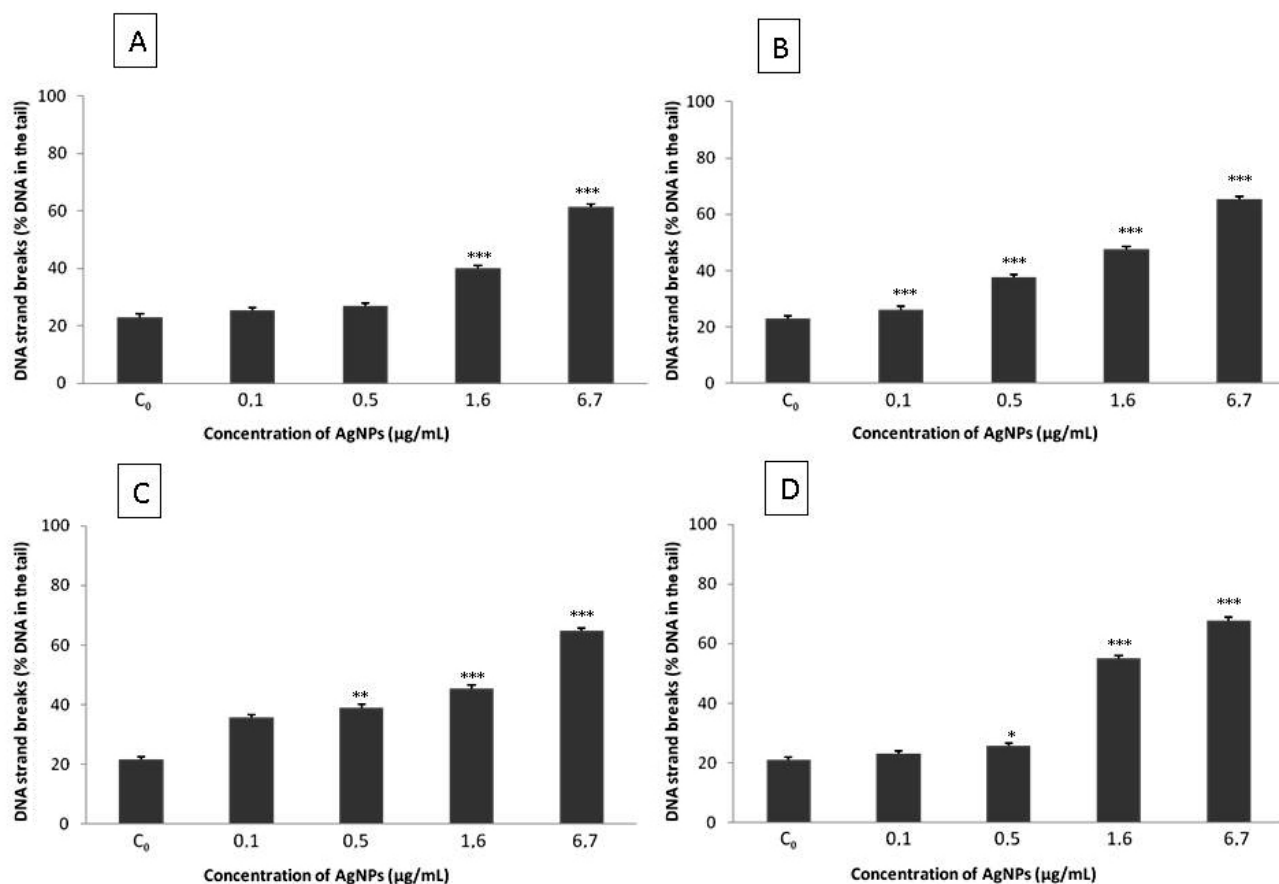


Fig. 2. DNA strand breaks in HepG2 (A), HL-60 (B), NHDF (C) and HPF (D) cells exposed to AgNPs of 42 nm, as determined by comet assay. The results are expressed as the mean \pm SD of three independent experiments for data point of the % DNA in the tail of cells. C₀ – untreated cells without enzymes.

Asterisks indicate significant difference from the control *** P \leq 0.001, ** P \leq 0.01, * P \leq 0.05.

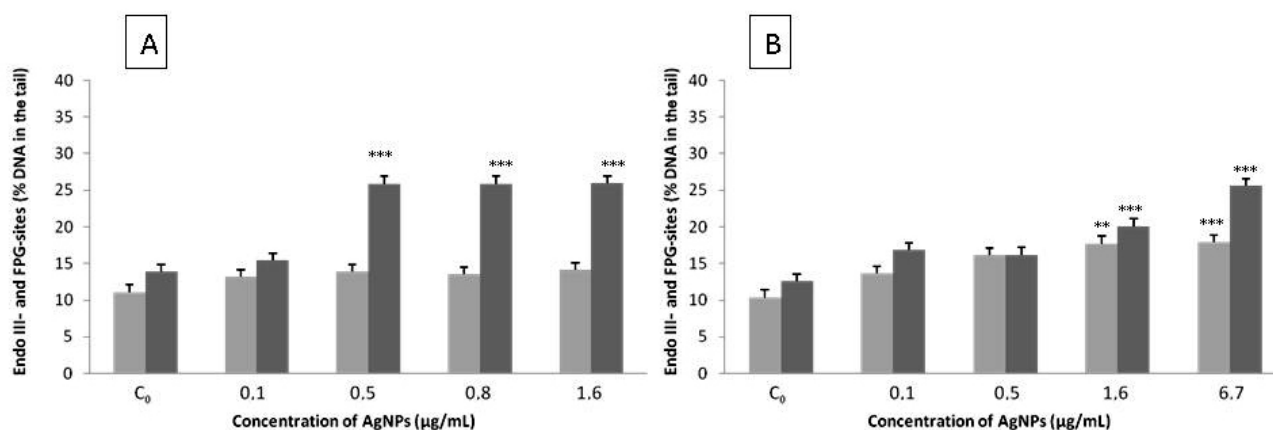


Fig. 3. Oxidative DNA damage, Endo III-sites (■) and Fpg-sites (■) in HepG2 cells exposed to AgNPs of 4.7 nm (A) and 42 nm (B), using the enzyme-modified comet assay. C₀ – untreated cells incubated with Endo III (■) and Fpg (■) enzymes. Asterisks indicate significant difference from the control *** P \leq 0.001, ** P \leq 0.01.

oxidized pyrimidines compared to the control. However, a significant increase of oxidized purines was observed after the treatment with 0.5–1.6 $\mu\text{g ml}^{-1}$ AgNPs (12% increase of DNA in the tail compared to control) (Fig. 3A). In the treatment with 42 nm AgNPs, the concentrations of 1.6 and 6.7 $\mu\text{g ml}^{-1}$ caused a significant increase of Endo III- and Fpg-sites compared to the control (7.5%

and 7.5–13% increase of DNA in the tail compared to control, respectively) (Fig. 3B).

Oxidative DNA damage induced by 4.7 nm coated and 42 nm uncoated AgNPs in HL-60 cells incubated with Endo III and Fpg enzymes is shown in Fig. 4. A significant increase of oxidized pyrimidines (9.4% increase in DNA in the tail compared to control) was only

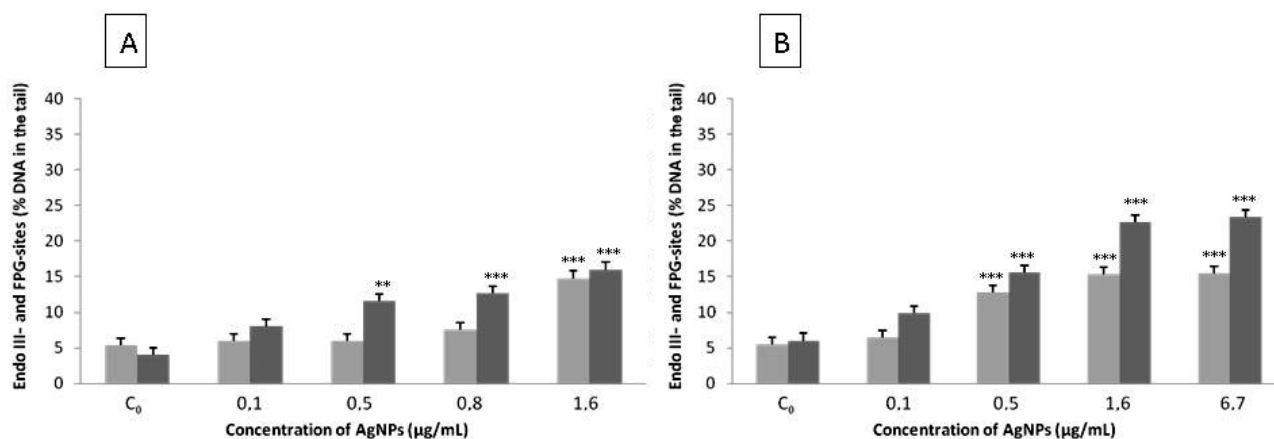


Fig. 4. Oxidative DNA damage, Endo III-sites (■) and Fpg-sites (■) in HL-60 cells exposed to AgNPs of 4.7 nm (A) and 42 nm (B), using the enzyme-modified comet assay. C_0 – untreated cells incubated with Endo III (■) and Fpg (■) enzymes. Asterisks indicate significant difference from the control *** $P \leq 0.001$, ** $P \leq 0.01$.

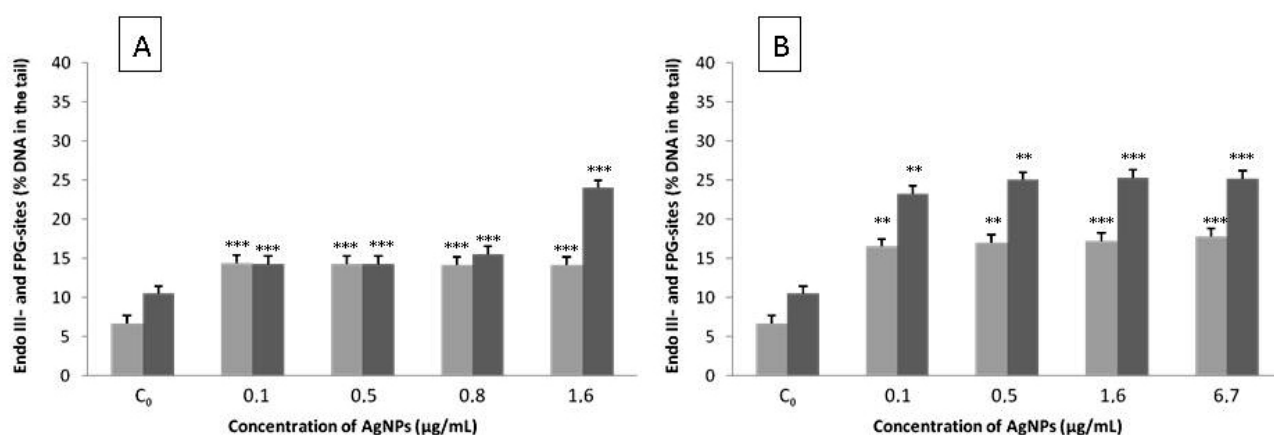


Fig. 5. Oxidative DNA damage, Endo III-sites (■) and Fpg-sites (■) in NHDF cells exposed to AgNPs of 4.7 nm (A) and 42 nm (B), using the enzyme-modified comet assay. C_0 – untreated cells incubated with Endo III (■) and Fpg (■) enzymes. Asterisks indicate significant difference from the control *** $P \leq 0.001$, ** $P \leq 0.01$.

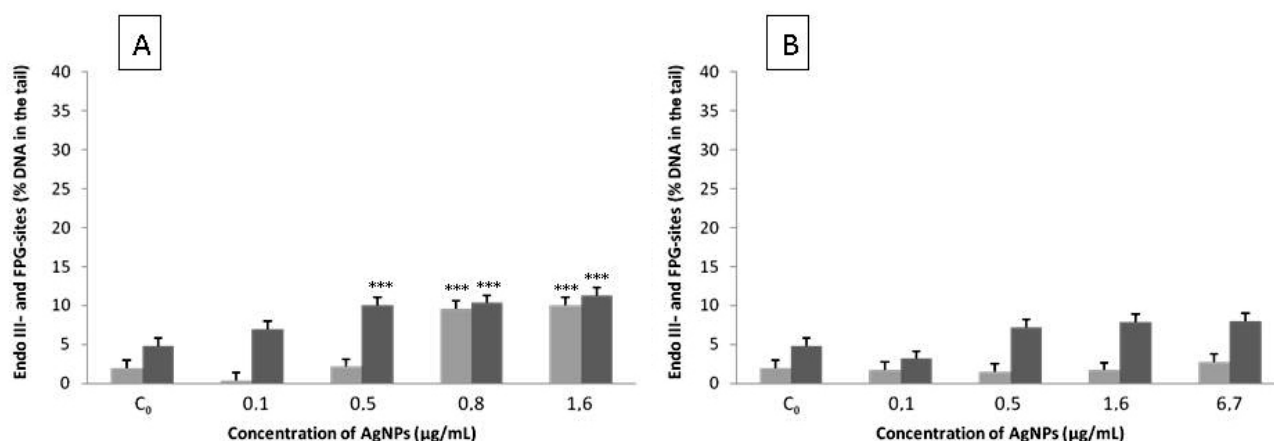


Fig. 6. Oxidative DNA damage, Endo III-sites (■) and Fpg-sites (■) in HPF cells exposed to AgNPs of 4.7 nm (A) and 42 nm (B), using the enzyme-modified comet assay. C_0 – untreated cells incubated with Endo III (■) and Fpg (■) enzymes. Asterisks indicate significant difference from the control *** $P \leq 0.001$.

observed at the highest concentration of 4.7 nm coated AgNPs, while oxidized purines were found at 0.5–1.6 $\mu\text{g ml}^{-1}$ (7.6–12 % increase in DNA in the tail compared to control, respectively)(Fig. 4A). With 42 nm uncoated AgNPs, a significant increase of Endo III- and Fpg-sites

was found at concentrations of 0.5–6.7 $\mu\text{g ml}^{-1}$ (7.3–10 % and 9.5–17.3 % increase in DNA in the tail compared to control, respectively)(Fig. 4B).

Figure 5 shows the oxidative DNA damage, Endo III- and Fpg-sites, in NHDF cells exposed to 4.7 nm and 42 nm

uncoated AgNPs. Coated AgNPs of 4.7 nm (Fig. 5A) significantly increased the number of Endo III-sites compared to the control at all tested doses (0.1–1.6 $\mu\text{g ml}^{-1}$; 7.5% increase in DNA in the tail compared to control). Oxidized purines were also observed at all concentrations, but the maximum formation of Fpg sites was found at 1.6 $\mu\text{g ml}^{-1}$ (13.5% increase in DNA in the tail compared to control). The large 42 nm uncoated AgNPs (Fig. 5B) induced oxidation of pyrimidines and purines at all tested doses (9.5% and 14.5% increase in DNA in the tail compared to control, respectively).

Finally, in HPF cells the treatment with 4.7 nm coated AgNPs (Fig. 6A) showed a significant increase in formation of Endo III-sites at 0.8–1.6 $\mu\text{g ml}^{-1}$ (7% increase in DNA in the tail compared to control). However, the formation of Fpg-sites was found at concentrations of 0.5–1.6 $\mu\text{g ml}^{-1}$ (5.2–6.5% increase in DNA in the tail compared to control, respectively). Uncoated AgNPs of 42 nm did not show any oxidative DNA damage. No significant increase in the formation of Endo III- and Fpg-sites (Fig. 6B) was found.

Benzo(a)pyrene (100 mM) used as positive control induced numbers of Endo III- and Fpg-sites 1.77–1.75 (HepG2), 2.30–2.38 (HL-60), 2.00–1.53 (NHDF) and 3.23–2.93 (HPF) fold higher than the background values, respectively (data not shown).

Discussion

AgNPs, which have antibacterial properties, have been integrated into hundreds of consumer products. Consequently, industry workers, consumers and environment are anticipated to be increasingly exposed to AgNPs. The potential routes of human exposure are by oral administration, intravenous injection, dermal contact and inhalation; for this reason, HepG2, HL-60, NHDF and HPF cells were used in the present study. Hepatoma cells (HepG2) were used because the liver is a primary site of AgNP accumulation following exposure (Johnston et al., 2010); leukaemia cells (HL-60) were used to investigate the effect of AgNPs on blood cells; dermal fibroblasts (NHDF) and pulmonary fibroblasts (HPF) were employed to consider the implication of dermal exposure to AgNPs (due to the exploitation of these particles within wound dressings) and to evaluate the pulmonary genotoxicity of AgNPs often focused on the response of epithelial cells that line the airways or alveoli (due to their prominent role in the particle clearance, Johnston et al., 2010).

Many studies in the area of nanotoxicology have focused on cytotoxicity. However, such effects often occur first at rather high concentrations, and the subtle effects that arise at lower concentrations, without necessarily causing cell death, also need to be considered. Previous studies have demonstrated that the mechanism of AgNP toxicity involves disruption of the mitochondrial respiratory chain, leading to production of reactive oxygen species (ROS) and interruption of ATP synthesis, which in turn causes DNA damage (Arora et al., 2008; Fold-

bjerg, 2009). One of the most important effects is damage to DNA, since an increased genetic instability is associated with cancer development (Karlsson, 2010). Genotoxicity evaluation is an ideal assessment of biosafety at the molecular level for nanomaterials. There are no standardized testing methods for the genotoxicity of nanoparticles; however, the comet assay is a highly sensitive method and widely applied in nanotoxicological studies about genotoxicity (Karlsson, 2010). In the review by Landsiedel et al. (2009), the comet assay was more sensitive and frequently used to confirm the genotoxicity of nanoparticles than the well-known Ames test in bacterial systems. Moreover, recent reviews have concluded that genotoxicity of nanomaterials is still inadequate for general conclusions (Cunningham, 2007; Landsiedel et al., 2009). In the present work, we conducted the comet assay to evaluate the genotoxicity of AgNPs of 4.7 nm and 42 nm in HepG2, HL-60, NHDF and HPF cells.

Prior to the genotoxicity studies, our research reported nanoparticle characterization and cytotoxicity of AgNPs of 4.7 and 42 nm in HepG2, HL-60, NHDF and HPF cells (Ávalos et al., 2014a, b). Our results showed that the particle size agrees well with the particle size in different AgNPs specified by the manufacture. AgNPs formed agglomerates in the cell medium, which were larger than the primary particle sizes. In addition, AgNPs of 4.7 nm and 42 nm exhibited a dramatic difference in cytotoxicity. Small AgNPs were much more cytotoxic than the large ones in all the cell types used. However, no cytotoxicity was previously found at the concentrations of AgNPs tested in the present work. Cell viability was always above 80 % of control viability.

In the present work, we used exposure to non-cytotoxic concentrations in the range of 0.1–1.6 $\mu\text{g ml}^{-1}$ (AgNPs 4.7 nm) and 0.1–6.7 $\mu\text{g ml}^{-1}$ (AgNPs 42 nm), based on previous studies of AgNPs against these human cells (Ávalos et al., 2014a, b). The results obtained in the comet assay indicated that both sizes of AgNPs were able to cause a significant and dose-dependent increase in DNA damage (strand breaks) after 24 h of treatment in HepG2, HL-60, NHDF and HPF cells. Our data are in agreement with several *in vitro* studies using different sizes of AgNPs (5–260 nm) that have indicated genotoxicity effects in different types of human and mammalian cells (Ahamed et al., 2008; AshaRani et al., 2009; Kawata et al., 2009; Foldbjerg et al., 2011; Hackenberg et al., 2011; Kim et al., 2011; Flower et al., 2012; Li et al., 2012; Nymark et al., 2013). The most common effects considered in these studies include: DNA strand breaks, micronuclei induction and chromosomal aberrations, but not oxidative DNA damage. In the present study, the difference in the cellular response to AgNPs was also compared. Our results showed that DNA damage was similar in all cell lines, although HepG2 cells were the most resistant to DNA strand breaks after the treatment with 4.7 nm coated and 42 nm uncoated AgNPs (2.22 and 2.65-fold higher than control, respectively). Kawata et al. (2009) demonstrated

that exposure to $1.0 \mu\text{g ml}^{-1}$ of AgNPs (7–10 nm in size) induced micronucleation frequency (MNF) up to 47.9% in HepG2 cells. In our study, HPF cells showed the greatest proportion of DNA strand breaks compared to the control after the treatment with 4.7 nm coated and 42 nm uncoated AgNPs (3.09 and 3.24-fold, respectively) (Figs. 1D, 2D). In a study by Nymark et al. (2013), the genotoxic effects of AgNPs (42.5 nm) coated with PVP were investigated in a human bronchial epithelial cell line. DNA damage detected by the comet assay was seen after 4 and 24 h exposures and the induction was also dose-dependent. Accordingly, Kim et al. (2011) found that AgNPs (43–260 nm) stimulated DNA breakage and micronuclei formation in a dose-dependent manner in BEAS-2B cells. In another study, the comet assay test showed DNA damage in human mesenchymal stem cells after 1, 3 and 24 h at AgNP (< 50 nm) concentrations from 0.1 – $10 \mu\text{g ml}^{-1}$ (Hackenberg et al., 2011).

Our previous studies have also reported membrane leakage (LDH) and inhibition of mitochondrial activity (MTT) upon 4.7 and 42 nm AgNP exposure in different cell lines (HepG2, HL-60, NHDF and HPF) (Ávalos et al., 2014a,b). In all toxicity endpoints studied, 4.7 nm AgNPs were much more toxic than the large ones (42 nm). The particle size has been reported to influence toxicity (Cha et al., 2008; Hsin et al., 2008). In this work, the DNA strand breaks were also size-dependent, since 4.7 nm coated AgNPs ($1.6 \mu\text{g ml}^{-1}$) showed higher percentage of DNA in the tail than 42 nm uncoated AgNPs. In accord with our data, Park et al. (2011) also observed that AgNPs of 20 nm were more genotoxic than AgNPs of 80 nm and 113 nm in embryonic fibroblasts (MEF-LacZ). However, Gliga et al. (2014) demonstrated, using the comet assay, that in contrast to the size-dependent effect on lung cell viability, all tested AgNPs (10, 40 and 75 nm) induced similar DNA damage after 24 h.

In the present work, in addition to assessing the damage to DNA (strand breaks), we also evaluated the oxidative DNA damage induced by AgNPs (4.7 nm coated and 42 nm uncoated) in HepG2, HL-60, NHDF and HPF cells. To this end, oxidatively damaged bases were detected by the comet assay by adding two repair-specific enzymes, endonuclease III and Fpg, which are able to recognize the oxidized pyrimidines and purines, respectively. Our results showed that AgNPs of 4.7 nm induced a significant increase of oxidation of pyrimidines (except in HepG2) and purines compared to the control in all cell lines (Figs. 3A, 4A, 5A and 6A). Moreover, AgNPs of 42 nm also significantly increased oxidation of the pyrimidines and purines compared to the control in HepG2, HL-60 and NHDF cells (Figs. 3B, 4B and 5B). However, 42 nm uncoated AgNPs did not cause any oxidative DNA damage in any of the concentrations used in HPF cells (Fig. 6B). Kim et al. (2011) observed that AgNPs (43–260 nm) induced oxidation of DNA bases in human normal bronchial epithelial cells. In another study with AgNPs of 5 nm, Mei et al. (2012) observed oxidation of pyrimidines and purines in mouse lymphoma cells by the oxidative stress comet assay.

Our results showed that the oxidative DNA damage by AgNPs was not size-dependent, but depended on the cell line. NHDF and HL-60 cells were the most sensitive to oxidized purines and pyrimidines induced by both AgNP sizes. However, HPF was the most resistant to the oxidative DNA damage induced by 42 nm AgNPs and HepG2 to the oxidized pyrimidines induced by 4.7 nm AgNPs. Different cellular responses related to oxidative DNA damage could be due to the diverse genetic background of human cells (Foldbjerg and Autrup, 2013).

Furthermore, our results showed that in all treatments purines were more oxidized than pyrimidines. This result is consistent with the reports that purines are more vulnerable targets to oxidative DNA damage than pyrimidines, because the pyrimidines can be rapidly repaired by transferring an electron to their purine counterpart (Jovanovic et al., 1986). The induction of DNA breaks by addition of Endo III and Fpg indicates that the DNA damage resulting from AgNP treatments mainly consisted in oxidized nucleotides.

Panda et al. (2011) observed that the DNA damage induced by AgNPs was prevented by Tiron and dimethyl thiourea that scavenge O_2^- and H_2O_2 , respectively. ROS scavengers, especially superoxide dismutase (SOD), could reduce the genotoxic effects, thereby implicating oxidative stress as a mechanism (Kim et al., 2011). These findings demonstrated the role of ROS in the AgNP-induced DNA damage. The mechanism of action by which AgNPs cause DNA damage is not fully understood. One of the plausible mechanisms by which AgNPs may cause DNA damage is via generation of free radicals (Kim et al., 2011; Foldbjerg and Autrup, 2013). Several *in vitro* studies have demonstrated cellular responses related to oxidative stress after AgNP exposure. Reactive oxygen intermediates are formed when oxidative dissolution of AgNPs occurs, suggesting a direct NP-mediated mechanism (Liu and Hurt, 2010). In previous studies, cytotoxicity induced by 4.7 and 42 nm AgNPs was efficiently prevented by N-acetyl-L-cysteine treatment, which suggested that oxidative stress was primarily responsible for the cytotoxicity of AgNPs. In addition, our previous results also demonstrated that 4.7 nm coated and 42 nm uncoated AgNPs caused an increase in generation of ROS, drastic glutathione depletion and slight, but not statistically significant, inactivation of SOD, and consequently oxidative stress in HepG2, HL-60, NHDF and HPF cells (Ávalos et al., 2014a, b). Thus, genotoxic effects induced by AgNP exposure may occur in human cells, and different modes of action could be involved. ROS produced by exposure to AgNPs could interact with and damage proteins or DNA. It is also possible that AgNPs interact directly with proteins or DNA and cause genotoxic effects (Foldbjerg and Autrup, 2013). Moreover, apart from the damaging effects to cellular proteins, lipids and DNA, an increasing level of ROS triggers the cell to respond by activating pro-inflammatory signalling cascades, and ultimately induces programmed cell death (Nel et al., 2006).

In conclusion, our study showed that 4.7 nm coated and 42 nm uncoated AgNPs induced DNA strand breaks in a dose- and size-dependent manner in human hepatoma and leukaemia cells and in human dermal and pulmonary fibroblasts, as detected by the alkaline comet assay. The smaller AgNPs (4.7 nm) were more genotoxic than the 42 nm AgNPs. Furthermore, the genotoxicity of both AgNPs was also dependent on the cell line, with human pulmonary fibroblasts showing the highest DNA damage. Moreover, 4.7 nm and 42 nm AgNPs were able to cause oxidative DNA lesions (measured as Endo III- and Fpg-sites). However, the oxidative damage was not size-dependent, only differences were observed between the cell lines. HL-60 and NHDF cells showed the greatest oxidative DNA damage; in contrast, HPF cells were the most resistant to Endo III and Fpg oxidation. Thus, the risk of being exposed to silver nanoparticles depends on a number of factors, including exposed cell type, silver nanoparticle size, and likely surface chemistry. Deriving safe exposure limits for silver nanoparticles should therefore be handled by a case-by-case approach. This implies that care has to be taken while processing and formulating nanoparticles until their final, finished product.

References

- Ahamed, M., Karns, M., Goodson, M., Rowe, J., Hussain, S. M., Schlager, J. J., Hong, Y. (2008) DNA damage response to different surface chemistry of silver nanoparticles in mammalian cells. *Toxicol. Appl. Pharmacol.* **233**, 404-410.
- Ahamed, M., Posgai, R., Gorey, T. J., Nielsen, M., Hussain, S. M., Rowe, J. J. (2010) Silver nanoparticles induced heat shock protein 70, oxidative stress and apoptosis in *Drosophila melanogaster*. *Toxicol. Appl. Pharmacol.* **242**, 263-269.
- Arora, S., Jain, J., Rajwade, J. M., Paknikar, K. M. (2008) Cellular responses induced by silver nanoparticles: *in vitro* studies. *Toxicol. Lett.* **179**, 93-100.
- Asharani, P. V., Grace, L. K. M., Hande, M. P., Aliyaveetil, S. (2009) Cytotoxicity and genotoxicity of silver nanoparticles in human cells, *ACS Nano* **3**, 279-290.
- Ávalos, A., Haza, A. I., Mateo, D., Morales, P. (2014a) Cytotoxicity and ROS production of manufactured silver nanoparticles of different sizes in hepatoma and leukemia cells. *J. Appl. Toxicol.* **34**, 413-423.
- Ávalos, A., Haza, A. I., Mateo, D., Morales, P. (2014b) Interactions of manufactured silver nanoparticles of different sizes with normal human dermal fibroblasts. *Int. Wound J.* **25**, doi: 10.1111/iwj.12244.
- Boiteux, S. (1993) Properties and biological functions of the NTH and FPG proteins of *Escherichia coli*: two DNA glycosylases that repair oxidative damage in DNA. *J. Photochem. Photobiol. B Biol.* **19**, 87-96.
- Cha, K., Hong, H. W., Choi, Y. G., Lee, M. J., Park, J. H., Chae, H. K., Ryu, G., Myung, H. (2008) Comparison of acute responses of mice livers to short-term exposure to nano-sized or micro-sized silver particles. *Biotechnol. Lett.* **30**, 1893-1899.
- Chen, X., Schluesener, H. J. (2008) Nanosilver: a nanoparticle in medical application. *Toxicol. Lett.* **176**, 1-12.
- Collins, A. R., Duthie, S. J., Dobson, V. L. (1993) Direct enzymic detection of endogenous oxidative base damage in human lymphocyte DNA. *Carcinogenesis* **14**, 1733-1735.
- Colvin, V. L. (2003) The potential environmental impact of engineered nanomaterials. *Nat. Biotechnol.* **21**, 1166-1170.
- Cunningham, M. J. (2007) Gene-cellular interactions of nanomaterials: genotoxicity to genomics. In: *Nanotoxicology: Characterization, Dosing and Health Effects*, eds. Monteiro-Riviere, N. A., Lang Tran, C., pp. 173-196, Informa Healthcare, New York.
- Doetsch, P. W., Henner, W. D., Cunningham, R. P., Toney, J. H., Helland, D. E. (1987) A highly conserved endonuclease activity present in *Escherichia coli*, bovine, and human cells recognizes oxidative DNA damage at sites of pyrimidines. *Mol. Cell Biol.* **7**, 26-32.
- European Commission (2012) Nanomaterials: Commission proposes case by case approach to assessment. *MEMO*, **12**, 732.
- Flower, N. A., Brabu, B., Revathy, M., Gopalakrishnan, C., Raja, S. V. K., Murugan, S. S., Kumaravel, T. S. (2012) Characterization of synthesized silver nanoparticles and assessment of its genotoxicity potentials using the alkaline comet assay. *Mutat. Res.* **742**, 61-65.
- Foldbjerg, R., Olesen, P., Hougaard, M., Dang, D. A., Hoffmann, H. J., Autrup, H. (2009) PVP-coated silver nanoparticles and silver ions induce reactive oxygen species, apoptosis and necrosis in THP-1 monocytes. *Toxicol. Lett.* **190**, 156-162.
- Foldbjerg, R., Dang, D. A., Autrup, H. (2011) Cytotoxicity and genotoxicity of silver nanoparticles in the human lung cancer cell line, A549. *Arch. Toxicol.* **85**, 743-750.
- Foldbjerg, R., Autrup, H. (2013) Mechanisms of silver nanoparticle toxicity. *Arch. Bas. App. Med.* **1**, 5-15.
- Gliga, A. R., Skoglund, S., Wallinder, I. O., Fadeel, B., Karlsson, H. (2014) Size-dependent cytotoxicity of silver nanoparticles in human lung cells: the role of cellular uptake, agglomeration and Ag release. *Part. Fibre Toxicol.* **11**, 11-28.
- Godard, T., Deslandes, E., Lebailly, P., Vigreux, C., Poulain, L., Sichel, F., Poul, J. M., Gauduchon, P. (1999) Comet assay and DNA flow cytometry analysis of staurosporine-induced apoptosis. *Cytometry* **36**, 117-122.
- Hackenberg, S., Scherzed, A., Kessler, M., Hummel, S., Technau, A., Froelich, K., Ginzkey, C., Koehler, C., Hagen, R., Kleinsasser, N. (2011) Silver nanoparticles: evaluation of DNA damage, toxicity and functional impairment in human mesenchymal stem cells. *Toxicol. Lett.* **201**, 27-33.
- He, W., Zhou, Y. T., Wamer, W. G., Boudreau, M. D., Yi, J. J. (2012) Mechanisms of the pH dependent generation of hydroxyl radicals and oxygen induced by Ag nanoparticles. *Biomaterials* **33**, 7547-7555.
- Hsin, Y. H., Chen, C. F., Huang, S., Shih, T. S., Lai, P. S., Chueh, P. J. (2008) The apoptotic effect of nanosilver is mediated by ROS- and JNK-dependent mechanism involving the mitochondrial pathway in NIH3T3 cells. *Toxicol. Lett.* **179**, 130-139.
- Johnston, H. J., Hutchison, G., Christensen, F. M., Peters, S., Hankin, S., Stone, V. (2010) A review of the *in vivo* and *in*

- vitro toxicity of silver and gold particulates: particle attributes and biological mechanisms responsible for the observed toxicity. *Crit. Rev. Toxicol.* **40**, 328-346.
- Jovanovic, S. V., Simic, M. G. (1986) One-electron redox potentials of purines and pyrimidines. *J. Phys. Chem.* **90**, 974-978.
- Kawata, K., Osawa, M., Okabe, S. (2009) In vitro toxicity of silver nanoparticles at noncytotoxic doses to HepG2 human hepatoma cells. *Environ. Sci. Technol.* **43**, 6046-6051.
- Karlsson, H. L. (2010) The comet assay in nanotoxicology research. *Anal. Bioanal. Chem.* **398**, 651-666.
- Kim, H. R., Kim, M. J., Lee, S. Y., Oh, S. M., Chung, K. H. (2011) Genotoxic effects of silver nanoparticles stimulated by oxidative stress in human normal bronchial epithelial (BEAS-2B) cells. *Mutat. Res.* **726**, 129-135.
- Kreuter, J., Gelperina, S. (2008) Use of nanoparticles for cerebral cancer. *Tumori* **94**, 271-277.
- Landsiedel, R., Kapp, M. D., Schulz, M., Wiench, K., Oesch, F. (2009) Genotoxicity investigations on nanomaterials: methods, preparation and characterization of test material, potential artifacts and limitation – many questions, some answers. *Mutat. Res.* **681**, 241-258.
- Li, Y., Chen, D. H., Yan, J., Chen, Y., Mittelstaedt, R. A., Zhang, Y., Biris, A. S., Heflich, R. H., Chen, T. (2012) Genotoxicity of silver nanoparticles evaluated using the Ames test and in vitro micronucleus assay. *Mutat. Res.* **745**, 4-10.
- Lima, R., Seabra, A. B., Durán, N. (2012) Silver nanoparticles: a brief review of cytotoxicity and genotoxicity of chemically and biogenically synthesized nanoparticles. *J. Appl. Toxicol.* **32**, 867-879.
- Liu, J., Hurt, R. H. (2010) Ion release kinetics and particle persistence in aqueous nano-silver colloids. *Environ. Sci. Technol.* **44**, 2169-2175.
- Maurer-Jones, M. A., Lin, Y. S., Haynes, C. L. (2010) Functional assessment of metal oxide nanoparticle toxicity in immune cells. *ACS Nano* **4**, 3363-3373.
- Maynard, A. D., Kuempel, E. D. (2005) Airborne nanostructured particles and occupational health. *J. Nanopart. Res.* **7**, 587-614.
- Mei, N., Zhang, Y., Chen, Y., Guo, X., Ding, W., Ali, S. F., Biris, A. S., Rice, P., Moore, M. N., Chen, T. (2012) Silver nanoparticle-induced mutations and oxidative stress in mouse lymphoma cells. *Environ. Mol. Mutagen.* **53**, 409-419.
- Mukherjee, S. G., O'Claonadh, N., Casey, A., Chambers, G. (2012) Comparative *in vitro* cytotoxicity study of silver nanoparticle on two mammalian cells lines. *Toxicol. In Vitro* **26**, 238-251.
- Nel, A., Xia, T., Mädler, L., Li, N. (2006) Toxic potential of materials at the nanolevel. *Science* **311**, 622-627.
- Nymark, P., Catalan, J., Suhonen, S., Jarventaus, H., Birkedal, R., Clausen, P. A., Jensen, K. A., Vippola, M., Savolainen, K., Norppa, H. (2013) Genotoxicity of polyvinylpyrrolidone-coated silver nanoparticles in BEAS 2B cells. *Toxicology* **313**, 38-48.
- Oberdorster, G., Oberdorster, E., Oberdorster, J. (2005) Nanotoxicology: an emerging discipline evolving from studies of ultrafine particles. *Environ. Health Perspect.* **113**, 823-839.
- Olive, P. L., Wlodek, D., Durand, R. E., Banath, J. P. (1992) Factors influencing DNA migration from individual cells subjected to gel electrophoresis. *Exp. Cell. Res.* **198**, 259-267.
- Olive, P. L., Frazer, G., Banath, J. P. (1993) Radiation-induced apoptosis measured in TK6 human B lymphoblast cells using the comet assay. *Radiat. Res.* **136**, 130-136.
- Panda, K. K., Achary, V. M., Krishnaveni, R., Padhi, B. K., Sarangi, S. N., Sahu, S. N., Panda, B. B. (2011) *In vitro* biosynthesis and genotoxicity bioassay of silver nanoparticles using plants. *Toxicol. In Vitro* **25**, 1097-1105.
- Park, M. V. D. Z., Neigh, A. M., Vermeulen, J. P., de la Fonteyne, L. J. J., Verharen, H. W., Briedé, J. J., van Loveren, H., de Jong, W. H. (2011) The effect of particle size on the cytotoxicity, inflammation, developmental toxicity and genotoxicity of silver nanoparticles. *Biomaterials* **32**, 9810-9817.
- Su, J., Zhang, J., Liu, L., Huang, Y., Mason, R. P. (2008) Exploring feasibility of multicolored CdTe quantum dots for *in vitro* and *in vivo* fluorescent imaging. *J. Nanosci. Nanotechnol.* **8**, 1174-1177.
- Tan, W. B., Jiang, S., Zhang, Y. (2007) Quantum-dot based nanoparticles for targeted silencing of HER2/neu gene via RNA interference. *Biomaterials* **28**, 1565-1571.
- Wallace, W. E., Keane, M. J., Murray, D. K., Chisholm, W. P., Maynard, A. D., Ong, T. M. (2007) Phospholipid lung surfactant and nanoparticle surface toxicity: lessons from diesel soots and silicate dusts. *J. Nanopart. Res.* **9**, 23-38.
- Wijnhoven, S. W. P., Peijnenburg, W. J. G. M., Herberths, C. A., Hagens, W. I., Oomen, A. G., Heugens, E. H. W., Roszek, B., Bisschops, J., Gosens, I., Van De Meent, D., Dekkers, S., De Jong, W. H., van Zijverden, M., Sips, A. N. J. A. M., Geertsma, R. E. (2009) Nano silver – a review of available data and knowledge gaps in human and environmental risk assessment. *Nanotoxicology* **3**, 109-138.
- Xia, T., Kovoichich, M., Brant, J., Hotze, M., Sempf, J., Oberley, T., Sioutas, C., Yeh, J. I., Wiesner, M. R., Nel, A. E. (2006) Comparison of the abilities of ambient and manufactured nanoparticles to induce cellular toxicity according to an oxidative stress paradigm. *Nano Lett.* **6**, 1794-1807.
- Yoon, K. Y., Hoon, B. J., Park, J. H., Hwang, J. (2007) Susceptibility constants of *Escherichia coli* and *Bacillus subtilis* to silver and copper nanoparticles. *Sci. Total Environ.* **373**, 572-575.